A robust statistical estimation (RoSE) algorithm jointly recovers the 3D location and intensity of single molecules accurately and precisely

Hesam Mazidi, Arye Nehorai, Matthew D. Lew

Hesam Mazidi, Arye Nehorai, Matthew D. Lew, "A robust statistical estimation (RoSE) algorithm jointly recovers the 3D location and intensity of single molecules accurately and precisely," Proc. SPIE 10500, Single Molecule Spectroscopy and Superresolution Imaging XI, 105000E (20 February 2018); doi: 10.1117/12.2289994

SPIE.

Event: SPIE BiOS, 2018, San Francisco, California, United States

A Robust Statistical Estimation (RoSE) algorithm jointly recovers the 3D location and intensity of single molecules accurately and precisely

Hesam Mazidi[a], Arye Nehorai[a], Matthew D. Lew*[a]
[a]Department of Electrical and Systems Engineering, Washington University in St. Louis,
1 Brookings Drive, St. Louis, MO, USA 63130

ABSTRACT

In single-molecule (SM) super-resolution microscopy, the complexity of a biological structure, high molecular density, and a low signal-to-background ratio (SBR) may lead to imaging artifacts without a robust localization algorithm. Moreover, engineered point spread functions (PSFs) for 3D imaging pose difficulties due to their intricate features. We develop a Robust Statistical Estimation algorithm, called RoSE, that enables joint estimation of the 3D location and photon counts of SMs accurately and precisely using various PSFs under conditions of high molecular density and low SBR.

Keywords: single-molecule localization microscopy, multi-dimensional reconstruction algorithm, joint sparsity, joint location and brightness estimation, 3D super-resolution fluorescence microscopy

1. INTRODUCTION

Fluorescence imaging and spectroscopy have been workhorse technologies in biological laboratories since their inception[1]. Labeling a specific biomolecule with a small organic dye or fluorescent protein enables single copies of these biomolecules to be detected as bright objects against a dark background within living cells[2,3]. The recent development of super-resolved fluorescence microscopy[4–6] magnifies the power and utility of these tools, enabling images of biological structures to be created with resolution beyond the diffraction limit of light (~250 nm for visible light). Single-molecule localization microscopy (SMLM) achieves this resolution by repeatedly localizing individual blinking fluorophores over time. The capabilities of SMLM are further augmented by its three-dimensional (3D) variants[7], where the point spread function (PSF), or optical response to a point emitter, is specifically designed to give 3D information from a 2D image captured by a camera. Indeed, SMLM is part of a modern trend in optics[8,9] that integrates computational algorithms with physical hardware in order to improve imaging performance.

The attainable resolution of SMLM is limited by the precision of localizing an individual molecule, termed localization precision[10–12], from Poissonian shot noise due to the finite number of photons detected from each molecule. Modern SM localization algorithms are capable of achieving the theoretical limit of localization precision[13–15]. Localization precision can be improved by utilizing brighter fluorophores[16–18], reducing photobleaching[19,20], and reducing background fluorescence within a sample. Further, the number and spatial distribution of molecular blinking events on the target structure can also limit the quality of reconstructed SMLM images[21,22]. SMLM imaging performance is also limited by the accuracy of localizing an individual molecule. Localization bias can result from model PSF mismatch[23] (e.g., arising from anisotropic molecular emission[14,24,25]), optical aberrations[26], and the image-processing algorithm[27] utilized to localize each molecule.

Recently, algorithms capable of localizing multiple overlapping molecules[28–31] have been utilized to decrease the time needed to acquire an SMLM dataset. However, they are optimized for specific optical PSFs and are not readily adaptable to analyze others. Here, we develop RoSE to accurately and precisely estimate the 3D location and brightness of SMs from microscopes utilizing a variety of 3D PSFs.

2. ROBUST STATISTICAL ESTIMATION

2.1 Forward model

We assume that within each imaging frame, no two molecules emit within a certain neighborhood. Therefore, the continuous position of a single molecule can be mapped to a distinct grid point in object space, where each point is associated with a brightness and a set of position gradients. Importantly, our signal model explicitly handles sub-pixel

*mdlew@wustl.edu; phone 1-314-935-6790; fax 1-314-935-7500; lewlab.wustl.edu

Single Molecule Spectroscopy and Superresolution Imaging XI, edited by Jörg Enderlein, Ingo Gregor, Zygmunt Karol Gryczynski, Rainer Erdmann, Felix Koberling, Proc. of SPIE Vol. 10500, 105000E
 · doi: 10.1117/12.2289994

shifts in the position of a molecule, whereas conventional brightness-only signal models cannot. This joint signal model together with a first-order approximation result in a linear forward imaging model with a convex set of constraints on the molecular parameters to be estimated, denoted as $\boldsymbol{\mathcal{O}} \in \mathbb{R}^{N\times 4}$, given by:

$$\boldsymbol{g} = \boldsymbol{A}\boldsymbol{\gamma} \tag{1}$$

$$\boldsymbol{A} = \left[\Phi, \boldsymbol{G}_x, \boldsymbol{G}_y, \boldsymbol{G}_z\right] \tag{2}$$

$$\boldsymbol{\gamma} = [\boldsymbol{s}^T, \boldsymbol{s}^T \odot \Delta\boldsymbol{x}^T, \boldsymbol{s}^T \odot \Delta\boldsymbol{y}^T, \boldsymbol{s}^T \odot \Delta\boldsymbol{z}^T] = \left[\boldsymbol{s}^T, \boldsymbol{p}_x^T, \boldsymbol{p}_y^T, \boldsymbol{p}_z^T\right] \tag{3}$$

$$\boldsymbol{\mathcal{O}} = \begin{bmatrix} s_1 & \Delta x_1 & \Delta y_1 & \Delta z_1 \\ s_2 & \Delta x_2 & \Delta y_2 & \Delta z_2 \\ \vdots & \vdots & \vdots & \vdots \\ s_N & \Delta x_N & \Delta y_N & \Delta z_N \end{bmatrix} \tag{4}$$

$$\boldsymbol{\mathcal{C}} = \left\{ s_i \geq 0, -s_i r_j \leq p_{j,i} < s_i r_j,\ i \in \{1, \dots, N\}, j \in \{x, y, z\} \right\} \tag{5}$$

where $\boldsymbol{g} \in \mathbb{R}^m$ represents the vectorized noiseless image relayed by the microscope; $\Phi \in \mathbb{R}^{m\times N}$ demotes the PSF matrix sampled at grid points; $\boldsymbol{G}_x \in \mathbb{R}^{m\times N}$, $\boldsymbol{G}_y \in \mathbb{R}^{m\times N}$, and $\boldsymbol{G}_z \in \mathbb{R}^{m\times N}$ represent corresponding gradient matrices along x, y, and z, respectively; N is the number of object grid points; and m is the number of image pixels. Further, $\boldsymbol{s} \in \mathbb{R}^N$ is the vectorized brightness and $\Delta\boldsymbol{x} \in \mathbb{R}^N$, $\Delta\boldsymbol{y} \in \mathbb{R}^N$, and $\Delta\boldsymbol{z} \in \mathbb{R}^N$ are the corresponding gradient vectors ($\odot$ represents component-wise multiplication of two vectors). Additionally, $\boldsymbol{\mathcal{C}}$ represents the convex set of constraints for a box centered at each grid point i with side lengths $2r_x$, $2r_y$, and $2r_z$ (Figure 1(a)).

2.2 Structured deconvolution

We first apply a structured deconvolution program to identify single molecules from their overlapping images. Our key insight is that the brightnesses $\boldsymbol{s}$ and position gradients $\left(\boldsymbol{G}_x, \boldsymbol{G}_y, \boldsymbol{G}_z\right)$ corresponding to single molecules are jointly sparse. That is, if the brightness of a molecule associated with a grid point is zero, then the corresponding position gradients should also be zero. The structured deconvolution is then cast as an optimization problem:

$$\min_{\boldsymbol{\gamma}\in\mathcal{C}} \mathcal{L}(\boldsymbol{\gamma}, \boldsymbol{A}; \boldsymbol{g}, \boldsymbol{b}) + \lambda\|\gamma\|_{1,2} \tag{6}$$

where $\mathcal{L}(\cdot)$ is the Poisson negative log likelihood function, $\|\cdot\|_{1,2}$ denotes the mixed $\ell_{1,2}$ norm to enforce joint sparsity, $\boldsymbol{b} \in \mathbb{R}^m$ is the vectorized background, and λ is a penalty parameter.

Figure 1(b) illustrates a 2D example of two closely-spaced molecules with significantly overlapping images. The molecular parameters $\boldsymbol{\mathcal{O}}$ recovered by Eqn. (6) cannot resolve the brightness and position of the two molecules. However, examining the joint structure of $\boldsymbol{\mathcal{O}}$ reveals that the brightness-weighted position gradients converge to the positions of each molecule. To make this mapping precise, we define a tensor $\boldsymbol{\mathcal{G}}$, called GradMap, in which each pixel, termed the source coefficient, takes on a value in $[-1,1]$ that signifies the local degree of convergence to that pixel (Figure 1(c)). Notably, GradMap leverages the convergent symmetry of the position gradients and does not require a symmetric PSF profile. Thus, the number of molecules and their initial parameters $\boldsymbol{\mathcal{O}}$ are estimated from the local maxima of GradMap (Figure 1(d)).

2.3 Adaptive maximum likelihood

After identifying the correct number of molecules via structured deconvolution, the errors in the initial estimates of their parameters need to be refined, as conventional sparse deconvolution programs exhibit systematic bias[30]. Interestingly, the distance between the true molecular position and the sparse recovery solution could be larger than a few grid points (Figure 1(e)). To restore accuracy, RoSE adaptively updates the grid point closest to the current estimate of the molecule's position by maximizing adaptively a constrained maximum likelihood. This strategy enhances the accuracy of both molecular position and brightness and attains the limits of precision indicated by the Cramér-Rao bound (CRB)[32].

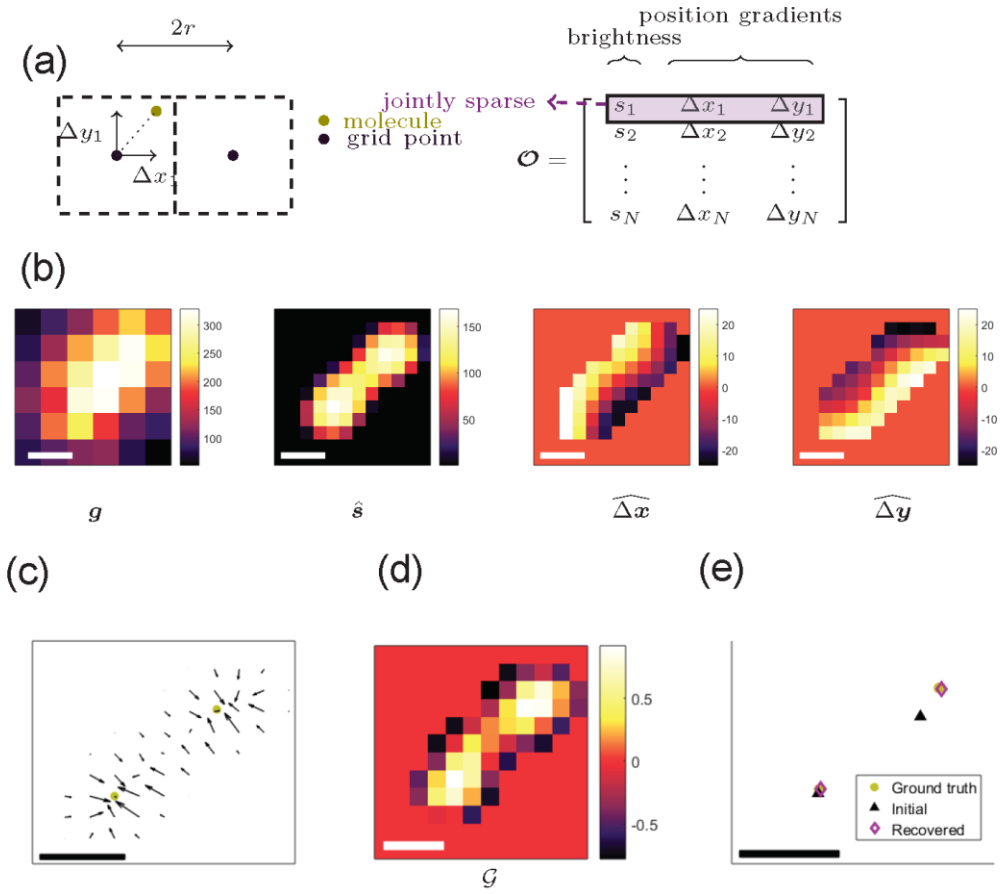

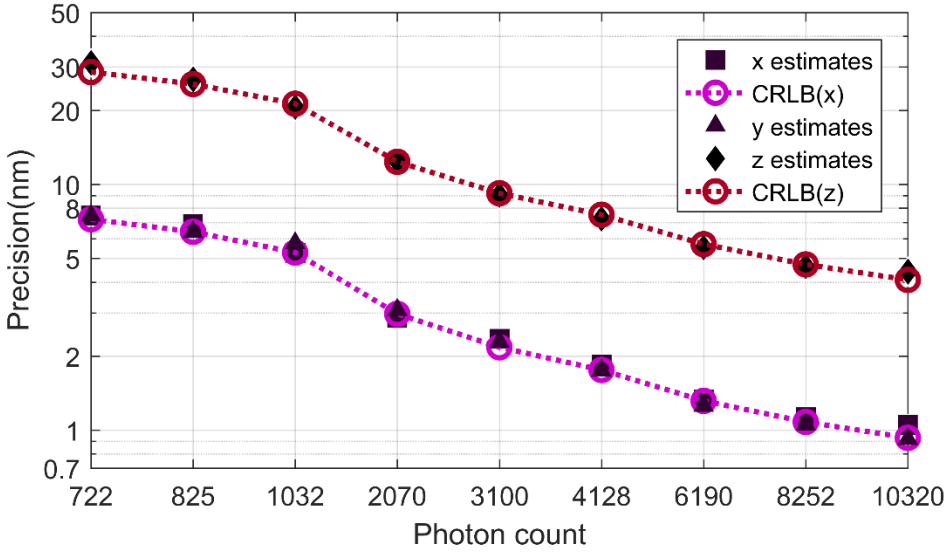

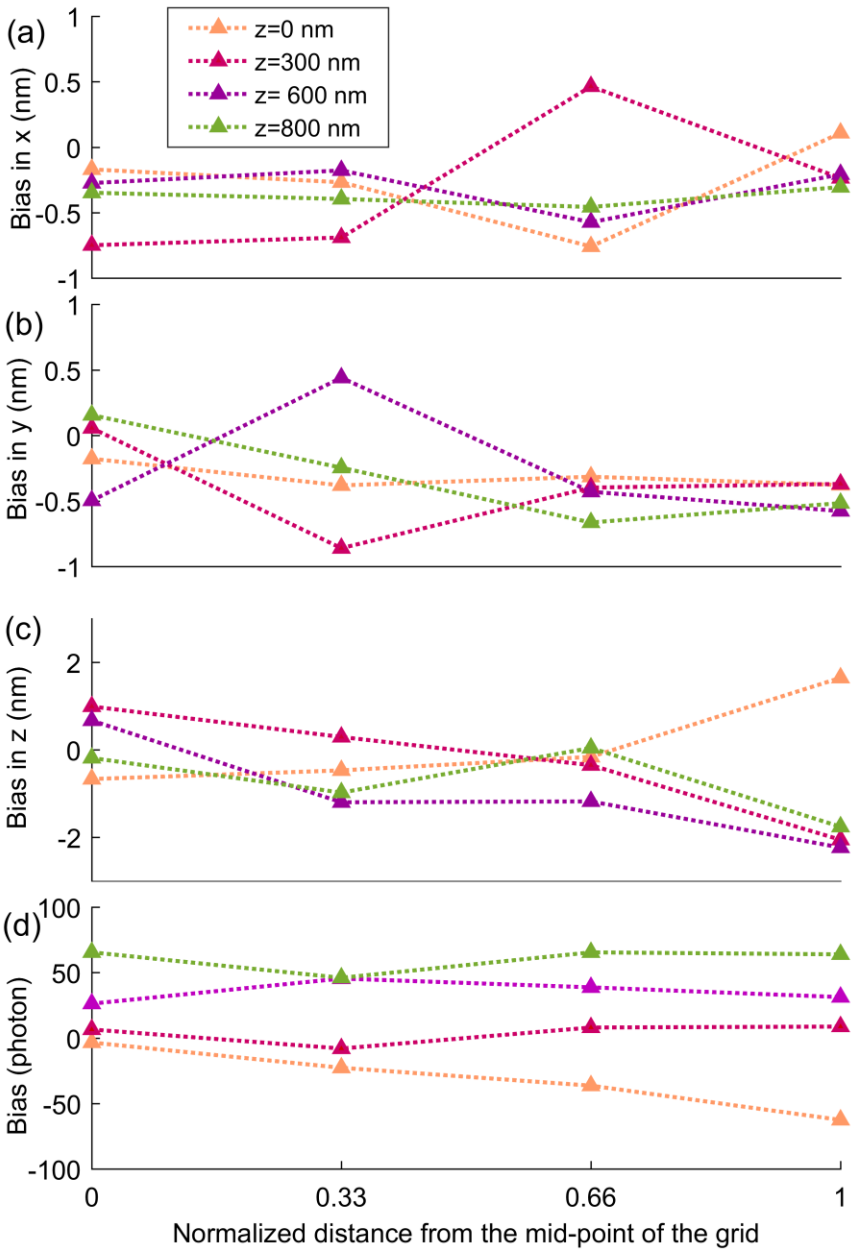

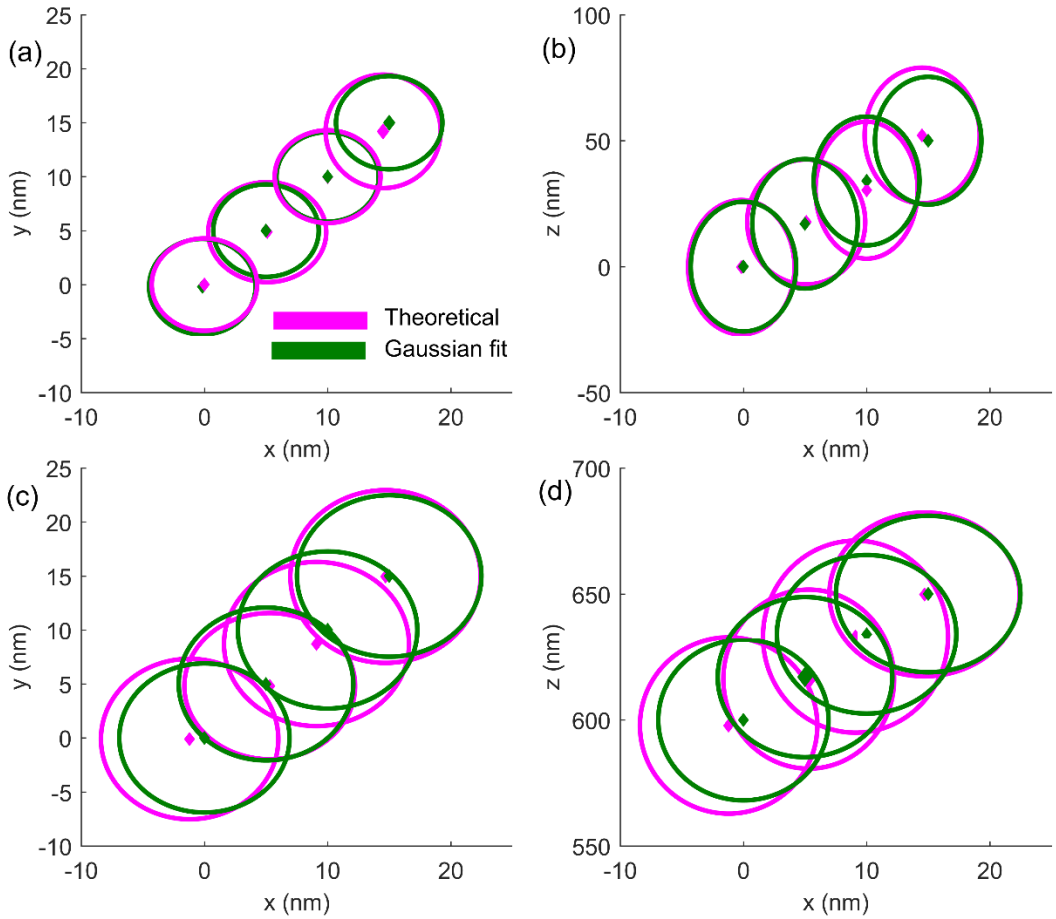

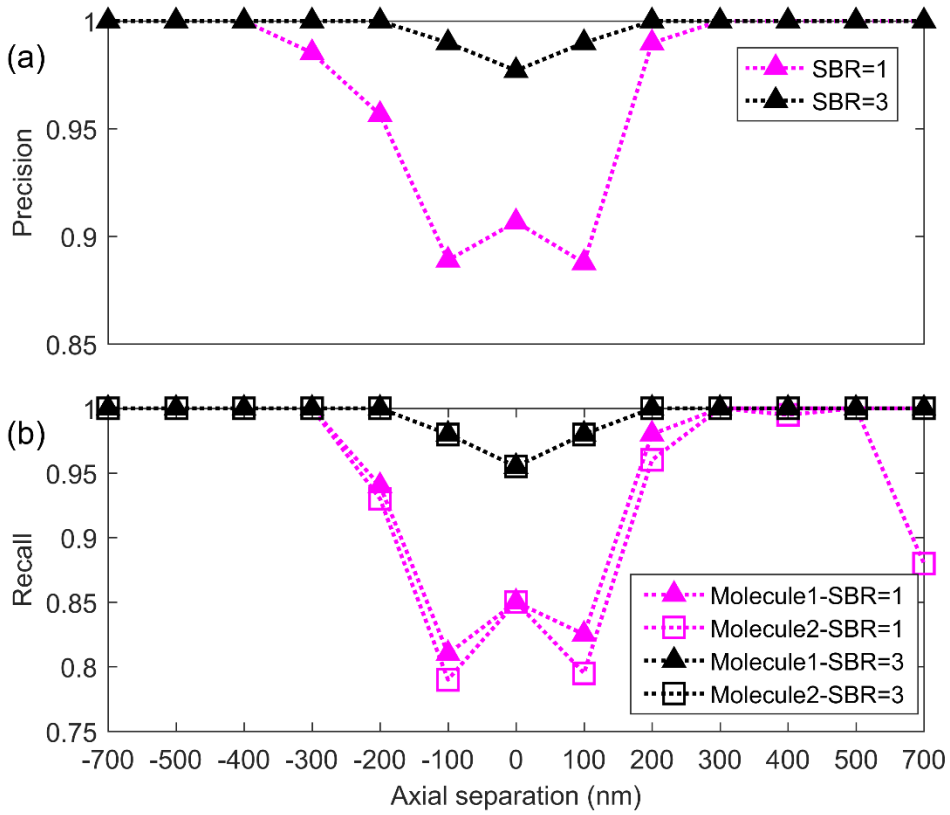

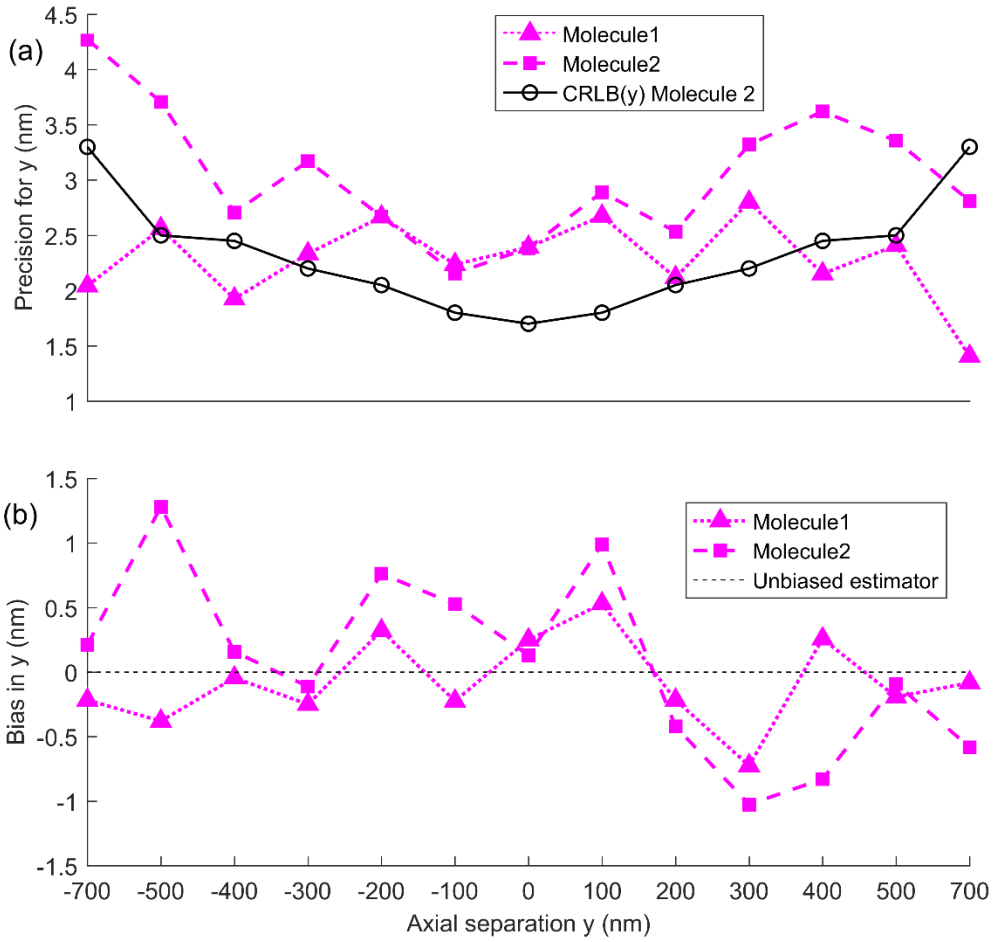

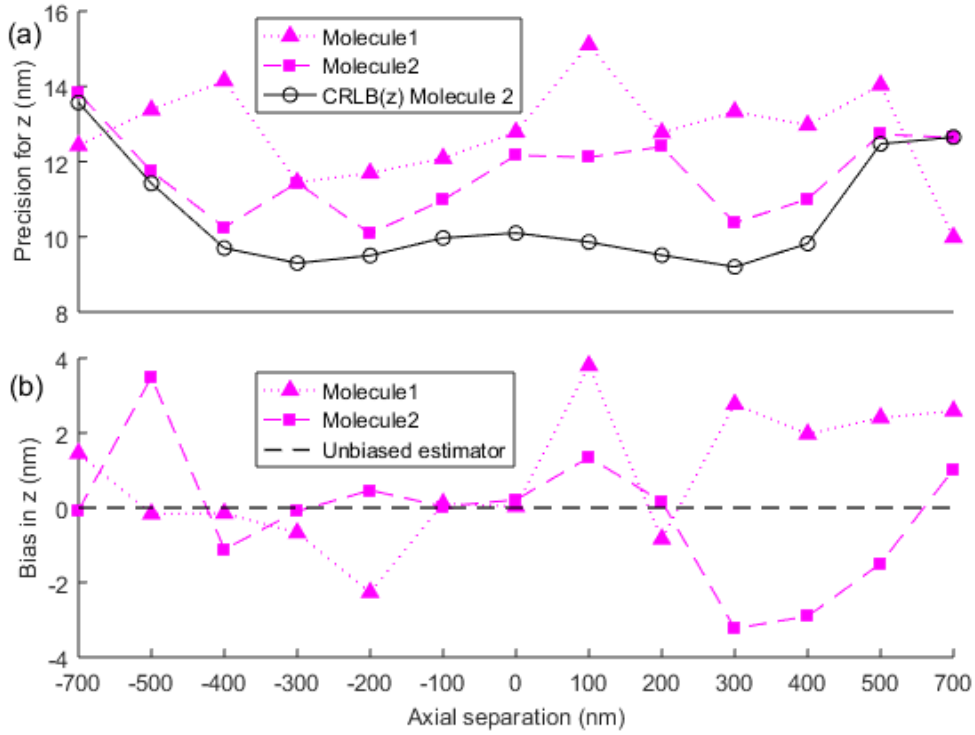

54(28), 8034–8053 (2015).
[5] Hell, S. W., "Nanoscopy with Focused Light (Nobel Lecture)," Angew. Chemie Int. Ed. **54**(28), 8054–8066 (2015).
[6] Moerner, W. E., "Single-Molecule Spectroscopy, Imaging, and Photocontrol: Foundations for Super-Resolution Microscopy (Nobel Lecture)," Angew. Chemie Int. Ed. **54**(28), 8067–8093 (2015).
[7] von Diezmann, A., Shechtman, Y. and Moerner, W. E., "Three-Dimensional Localization of Single Molecules for Super-Resolution Imaging and Single-Particle Tracking," Chem. Rev. **117**(11), 7244–7275 (2017).
[8] Zheng, G., Horstmeyer, R. and Yang, C., "Wide-field, high-resolution Fourier ptychographic microscopy," Nat. Photonics **7**(9), 739–745 (2013).
[9] McLeod, E. and Ozcan, A., "Unconventional methods of imaging: computational microscopy and compact implementations," Reports Prog. Phys. **79**(7), 76001 (2016).
[10] Thompson, R. E., Larson, D. R. and Webb, W. W., "Precise Nanometer Localization Analysis for Individual Fluorescent Probes," Biophys. J. **82**(5), 2775–2783 (2002).
[11] Ram, S., Ward, E. S. and Ober, R. J., "Beyond Rayleigh's criterion: a resolution measure with application to single-molecule microscopy.," Proc. Natl. Acad. Sci. U. S. A. **103**(12), 4457–4462 (2006).
[12] Rieger, B. and Stallinga, S., "The Lateral and Axial Localization Uncertainty in Super-Resolution Light Microscopy," ChemPhysChem **15**(4), 664–670 (2014).
[13] Abraham, A. V, Ram, S., Chao, J., Ward, E. S. and Ober, R. J., "Quantitative study of single molecule location estimation techniques," Opt. Express **17**(26), 23352 (2009).
[14] Mortensen, K. I., Churchman, L. S., Spudich, J. a and Flyvbjerg, H., "Optimized localization analysis for single-molecule tracking and super-resolution microscopy," Nat. Methods **7**(5), 377–381 (2010).
[15] Smith, C. S., Joseph, N., Rieger, B. and Lidke, K. a., "Fast, single-molecule localization that achieves theoretically minimum uncertainty," Nat. Methods **7**(5), 373–375 (2010).
[16] Dempsey, G. T., Vaughan, J. C., Chen, K. H., Bates, M. and Zhuang, X., "Evaluation of fluorophores for optimal performance in localization-based super-resolution imaging," Nat. Methods **8**(12), 1027–1036 (2011).
[17] Vaughan, J. C., Jia, S. and Zhuang, X., "Ultrabright photoactivatable fluorophores created by reductive caging," Nat. Methods **9**(12), 1181–1184 (2012).
[18] Wang, S., Moffitt, J. R., Dempsey, G. T., Xie, X. S. and Zhuang, X., "Characterization and development of photoactivatable fluorescent proteins for single-molecule-based superresolution imaging," Proc. Natl. Acad. Sci. **111**(23), 8452–8457 (2014).
[19] Rasnik, I., McKinney, S. a and Ha, T., "Nonblinking and long-lasting single-molecule fluorescence imaging.," Nat. Methods **3**(11), 891–893 (2006).
[20] Zheng, Q., Juette, M. F., Jockusch, S., Wasserman, M. R., Zhou, Z., Altman, R. B. and Blanchard, S. C., "Ultra-stable organic fluorophores for single-molecule research," Chem. Soc. Rev. **43**(4), 1044–1056 (2014).
[21] Shroff, H., Galbraith, C. G., Galbraith, J. A. and Betzig, E., "Live-cell photoactivated localization microscopy of nanoscale adhesion dynamics," Nat. Methods **5**(5), 417–423 (2008).
[22] Nieuwenhuizen, R. P. J., Lidke, K. a., Bates, M., Puig, D. L., Grünwald, D., Stallinga, S. and Rieger, B., "Measuring image resolution in optical nanoscopy," Nat. Methods **10**(6), 557–562 (2013).
[23] Deschout, H., Zanacchi, F. C., Mlodzianoski, M., Diaspro, A., Bewersdorf, J., Hess, S. T. and Braeckmans, K., "Precisely and accurately localizing single emitters in fluorescence microscopy," Nat. Methods **11**(3), 253–266 (2014).
[24] Engelhardt, J., Keller, J., Hoyer, P., Reuss, M., Staudt, T. and Hell, S. W., "Molecular Orientation Affects Localization Accuracy in Superresolution Far-Field Fluorescence Microscopy," Nano Lett. **11**(1), 209–213 (2011).
[25] Lew, M. D., Backlund, M. P. and Moerner, W. E., "Rotational mobility of single molecules affects localization accuracy in super-resolution fluorescence microscopy.," Nano Lett. **13**(9), 3967–3972 (2013).
[26] von Diezmann, A., Lee, M. Y., Lew, M. D. and Moerner, W. E., "Correcting field-dependent aberrations with nanoscale accuracy in three-dimensional single-molecule localization microscopy.," Optica **2**(11), 985–993 (2015).
[27] Sage, D., Kirshner, H., Pengo, T., Stuurman, N., Min, J., Manley, S. and Unser, M., "Quantitative evaluation of software packages for single-molecule localization microscopy," Nat. Methods **12**(8), 717–724 (2015).
[28] Holden, S. J., Uphoff, S. and Kapanidis, A. N., "DAOSTORM: an algorithm for high- density super-resolution microscopy," Nat. Methods **8**(4), 279–280 (2011).
[29] Zhu, L., Zhang, W., Elnatan, D. and Huang, B., "Faster STORM using compressed sensing," Nat. Methods **9**(7),

721–723 (2012).
[30] Min, J., Vonesch, C., Kirshner, H., Carlini, L., Olivier, N., Holden, S., Manley, S., Ye, J. C. and Unser, M., "FALCON: fast and unbiased reconstruction of high-density super-resolution microscopy data," Sci. Rep. **4**(1), 4577 (2015).
[31] Gustafsson, N., Culley, S., Ashdown, G., Owen, D. M., Pereira, P. M. and Henriques, R., "Fast live-cell conventional fluorophore nanoscopy with ImageJ through super-resolution radial fluctuations," Nat. Commun. **7**, 12471 (2016).
[32] Kay, S. M., [Fundamentals of statistical signal processing], Prentice Hall, Englewood Cliffs, N.J. (1993).
[33] Shechtman, Y., Weiss, L. E., Backer, A. S., Sahl, S. J. and Moerner, W. E., "Precise Three-Dimensional Scan-Free Multiple-Particle Tracking over Large Axial Ranges with Tetrapod Point Spread Functions," Nano Lett. **15**(6), 4194–4199 (2015).